Modular Active Payload Modules for Robotic Handlings in Future Orbital Missions

Wiebke Brinkmann[a]*, Marko Jankovic[b], Christoph Stoeffler[c], Gonzalo Guerra [d], Eduardo Urgoiti[e], Javier Vinals[f], Sebastian Bartsch[g]

German Research Center for Artificial Intelligence (DFKI), Robotics Innovation Center, Bremen, Germany,
[a]**wiebke.brinkmann@dfki.de, [b]marko.jankovic@dfki.de, [c]christoph.stoeffler@dfki.de, [g]sebastian.bartsch@dfki.de*
SENER Ingenieria y Sistemas, S.A., Spain,
[d]gonzalo.guerra@sener.es, [e]eduardo.urgoiti@sener.es, [f]javier.vinals@sener.es

* Corresponding Author

Abstract

The Low Earth Orbit is most easily accessible from Earth and has a low-energy state, therefore it has been the most exploited orbit since the dawn of spaceflight, resulting in alarming densities of man-made objects in certain regions. In order to avoid a future onset of a self-sustaining cascading process and provide more cost-effective access to space, the future of satellite operations will be asked for an option to reuse/refit existing on-orbit space assets instead of sending new ones. To this end the robotic on-orbit servicing/assembly of modular and reconfigurable systems represents one of the most mature and versatile technologies. Nevertheless, robotic servicing of a cooperative satellite is still an open research area facing many technical challenges, as it is evident by the amount of public/private funded projects in this area of research. One of those projects is the H2020 EU-funded project SIROM (Standard Interface for Robotic Manipulation of Payloads in Future Space Missions), which aims at developing an optimized multi-functional standard interface for mechanical, data, electrical and thermal connectivity. This interface in combination with modular and reconfigurable spacecraft units would allow modular spacecraft that would be upgraded/reconfigured at need via the so called Active Payload Modules (APM) which can be arbitrary payload elements, exchangeable subsystems, e.g. special processing units, tools and mechanisms for replacement of the module on-board. Within this context, this paper describes the APM concepts developed for on-orbit usage, their integration with the developed modular interface and planned testing. The core APM structure consists of a cube-shaped box of 150mm x 150mm x 150mm in size with the possibility to change the height. The APMs have easily detachable side panels and two interfaces per module for connection to other APMs or the manipulator's end-effector. The mass of an APM, consisting of a payload, two interfaces and core structure, is approximately 8,5kg. APM payloads will depend on the task of an APM. However, in our implementation one used payload will be a camera, which will take pictures of the test environment. This paper describes the development of the orbital APMs with a short overview about the SIROM interface by consideration of the requirements with selection of one concept for a final development, as well as lessons learned by verifications within first tests.
Keywords: space robotic, space interface, orbital missions, orbital payload, modularity

Acronyms/Abbreviations

Active Payload Module (APM), Electrical Ground Support Equipment (EGSE), Image-Based Visual Servo (IBVS), Interface (IF), Operational Grant (OG), Position-Based Visual Servo (PBVS), Standard Interface for Robotic Manipulation of Payloads in Future Space Missions (SIROM), SpaceWire (SpW).

1. Introduction

The 2016 call for the EU H2020 Strategic Research Cluster (SRC) in Space Robotics Technologies is an attempt to address the needs for reducing costs and increasing standardisation of space missions to allow access to space to a larger number of customers. The 2016 Call focus on the challenge of designing, manufacturing and testing of reliable and high performance common robotic building blocks for operation in space environments (orbital and/or planetary).

Six OGs have been awarded. This paper presents some of the intermediate results of the OG 5 SIROM project, targeting the realization of an integrated interface (with mechanical, data, electrical and thermal functionalities) that allows coupling of payload to robot manipulators and payload to other payload (or to a platform), for two different scenarios: space missions, and extra-terrestrial, planetary explorations. Thus, so called Active Payload Modules (APMs) are needed.

APMs are integral part of the SIROM development program. During this activity, they are conceptualized, designed and built with the main purpose of providing realistic operational environment for testing and verification of the SIROM interface. This process of test

and verification is envisaged to be done through realistic orbital and robotic planetary exploration scenarios, in which APMs play a central role. Two APMs for each track (two for orbital and two for planetary test scenarios) will be developed for testing the SIROM IF. Their design will not be space qualified but the essential for complying with the tests.

The orbital scenario missions aims to demonstrate the capabilities of SIROM to couple.

This paper describes the background and state of the art in robotic modularity and reconfigurability in space, also containing an overview of existing interfaces for connections of modules. The design principles and constrains shows given requirements for the interface and APMs. Section 4 explains the design of the orbital APM with its core elements and Section 5 describes first simulations and experiments. The paper then will be completed by a conclusion and outlook.

2. Background and state of the art

The importance and benefits of spacecraft modularity and reconfigurability can be found through the spaceflight history and were proven vital for the life extension of several Earth-orbiting spacecraft (e.g. the Hubble Space Telescope (HST) and SolarMax spacecraft) [1]. Moreover, it has enabled the assembly of large orbital structures, such as the International Space Station (ISS), that would otherwise be impossible to launch from ground.

The modularity and reconfigurability of a spacecraft or planetary rover in this paper defines the level of subdivision of its overall system in standardized and replaceable modules, connected with the main bus or interconnected between them via a standard interface [1].

The individual modules are envisioned to be able to contain any number of replaceable subsystems such as inertial reference units, payload, electronics, power distribution units, batteries, etc., that would otherwise be tightly integrated within the overall system [3].

Typical contemporary spacecraft/rover generally consists of a multitude of highly optimized and integrated components developed with cost and mass in mind not meant for serviceability nor reparability [1]. This monolithic design, enables the overall system to singlehandedly carry-out all the required mission tasks for an extended period but does not permit an easy way to upgrade the main platform on-ground and/or in orbit should some components fail or become obsolete [4].

In order to observe the benefits of modularity and reconfigurability, it is necessary to achieve the serviceable modularity or modularity at the component level as in case of the HST and ISS. In this case, the platform mainly consists of individual serviceable components integrated onto the main bus via a standard interface. Thus, allowing on-orbit reconfiguration of the system at the component level via tools and procedures specifically developed for each component separately due to the lack of serviceable modules [4].

This complication can be avoided by developing systems consisting of serviceable modules, i.e. having the degree of modularity at the subsystem level, which can be easily removed/replaced on-ground as well as in-orbit. Examples of such type of spacecraft are the Multimission Modular Spacecraft (MMS), the SolarMax spacecraft, and the Reconfigurable Operational spacecraft for Science and Exploration (ROSE). These spacecraft allow a great deal of flexibility both on-ground, during I&T activities, and in-orbit, while at the same time manage to keep the complexity of those tasks at the minimum [1].

Nevertheless, in order to enable future autonomous robotic on-orbit servicing and assembly an even greater degree of modularity is required. It can be observed in the intelligent Building blocks for On-orbit Servicing (iBOSS), Autonomous Assembly of a Reconfigurable Space Telescope (AAReST), DARPA's Satlets and Self Assembling Wireless Autonomous and Reconfigurable (SWARM). In these concepts, the overall spacecraft is composed out of compact interconnected modules, each with a limited functionality comparable to cells in a living organism. Each module is envisioned to be interconnected to another via an intelligent plug-and-play interface, allowing almost total in-orbit reconfiguration and assembly, with the highest level of flexibility in mind [1].

The type and number of individual modules shall be determined in advance based on an optimization process that will depend not only on engineering metrics, such as the cost and mass, but also on other less quantifiable metrics, such as future market uncertainties/projections and influence of stakeholders [2], [5], [6].

The goal of the SIROM project is to extend further this advanced modularity by providing a platform that could be used both in orbital and planetary environments with minimal adjustments.

2.1. Interfaces

To support the advanced modularity concepts mentioned in the previous subsection, over the years there has been a great variety of interfaces developed for space missions [7]. Among them, the four that deserve particular attention are: SINGO [8], Phoenix Satlet [9], DFKI's Electro-Mechanical Interface (EMI) [10], and iSSI (intelligent Satellite System Interface) [11].

SINGO is a fail-safe mechanical connector, powered by a single motor, which design allows two connectors to engage and disengage even if one does not cooperate.

The connector is made of four jaws that can bite those of the counterpart: one will bite from outside-in, while the other from inside-out [8].

The Phoenix Satlet interface is part of the DARPA's Phoenix project [12] which focuses on joining satlet modules to harvested sub-systems, such as an antenna, of defunct satellites, to create a new functioning space system [13]. The interface integrates electrical and mechanical functionalities for on-orbit attachment of tools [9].

EMI allows a higher level of modularity for planetary robots through the usage of Payload-Items (PLIs). This interface integrates a gender-principle approach to allow one side to be designed without any moving parts and openings where dust could enter. The EMI ensures mechanical connection and electrical and data transfer, as well as the possibility of visual servoing for an autonomous docking approach [14].

The iSSI interface, developed for the iBOSS project, is the only one that currently integrates four different functionalities in one single block: mechanical, thermal, data and electrical. In fact, the interface has a fail-safe hermaphroditic roto-lock mechanism, power contacts, a fiber optic data lens, and an annulus for thermal conductive exchange [11].

3. Design principles and constrains

The main design constrains the IF and orbital APMs have to comply are here presented:
- APMs are defined as containers with integrated subsystem or payload components, which can be used to fulfil a certain task (e.g. special sensor equipment or enhanced computation power).
- In the orbital application scenarios, APMs are mounted on a standard satellite platform or will be picked up by the end-effector of a robotic arm via the IF.
- These APMs are equipped with a suitable number of interfaces and a payload, which allows demonstrating a modular, maintainable spacecraft concept. The design of these APMs have the following properties:
  - At least two standard interfaces (SIROM) per module
  - Modules have different types of payload equipment inside. In the case of the orbital demonstration, this payload is a camera
  - Multiple usage (reusability)
  - Max. weight according to manipulator handling limit

- Arbitrary coupling between all integrated standard interfaces
- The SIROM APM shall consist of:
  - APM housing
  - APM payload
  - APM controller
  - SIROM controller
  - APM SW / FW
  - APM routing between the SIROM standard IF electrical, data, and thermal lines
  - Mounting provisions for at least two SIROM standard IF
  - Guiding aids to support mating and de-mating process

The SIROM standard robotic IF requires the following functionalities:
- to couple APMs with each other
- to couple the APM with the spacecraft platform mechanically and spacecraft data and power bus
- to couple with a compatible robotic manipulator
- to exchange data through a compatible robotic manipulator between the servicer and the APM
- to supply the APM with power while coupled to the manipulator

4. Design and core elements

The objective for the orbital scenario validation of SIROM is to demonstrate the successful transfer of an APM from an initial to a final operational location by means of a robot manipulator. The functioning of the interface of the APM with its payload and with the robot end-effector, as well as that of the end-effector with the robot manipulator will be validated. In this context two orbital APMs (APM-1 and APM-2) have been designed to support the orbital test scenarios.

4.1. Implemented device

The orbital APM-1 payload is a camera, see Figure 1, which will take pictures of the environment within the orbital test scenario. Commanded by the Electrical Ground Support Equipment (EGSE), it will ensure SIROM´s functionality. Its camera's operation will demonstrate:
- SIROM capability to transfer power loads (SIROM Power IF is in charge of switching on the camera)
- SIROM capability to transfer Data loads:
  - The camera will receive commands through CAN connectors

o The camera will send to the EGSE the pictures taken. The coupling must prove that the SpW retrieves the expected data package

Therefore, the APM-1 of orbital test scenario is the active APM of the demonstration. APM-1 consists of three core elements

- A SIROM IF on top of the APM. It is the SIROM IF to which the one SIROM IF of the end-effector of the robotic arm will be coupled.
- APM-1 structure and its payload (camera): In charge of taking the picture and send it in data packages via SpW to the EGSE through the lower end-effector SIROM IF or through the SIROM IF on top of the APM-2.
- A SIROM IF on the bottom of the APM-1 structure. It will be able to dock on the top side of the APM-2.
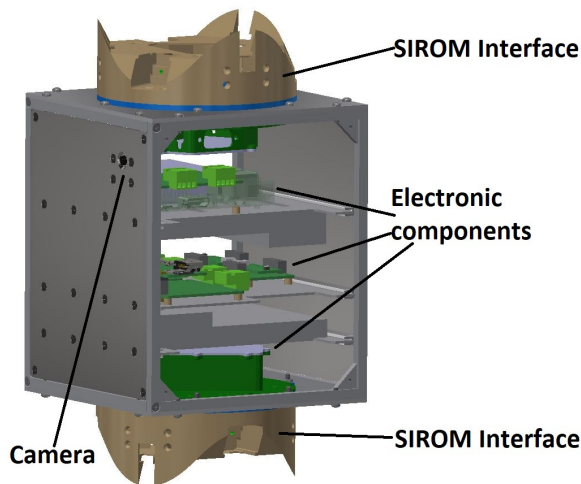
Figure 1 CAD model of APM-1 (credit: DFKI GmbH, SENER)

Apart from the core elements, APM-1 features SIROM Controllers (one per SIROM), which implement control of the actuators and the switches and will execute control algorithms and commands as well as send telemetry data. Although SIROM controller is accommodated inside the APM, it is important to mention that it is part of the SIROM interface not of the APM equipment. In addition the APM houses a controller, which implements control of the APM activity including activating, operating and managing the data of the camera. Furthermore power, data and thermal lines coming from the SIROM IF on top of APM-1 towards the bottom SIROM IF are connected to the different electronic components of the APM-1.

APM-2 is the passive APM of the orbital test demonstration. It is not equipped with any payload as it will not be used for any specific aspect. It will be a structure with one SIROM IF on the top of the APM and a mounting plate on the opposite side. This APM-2 will be permanently fixed on S/C target dummy and its SIROM will be permanently connected to the EGSE in order to allow for APM-1 data retrieval even when the robotic arm is not connected to the APM-1 through the end-effector.

One of the three core elements of APM-2 is one SIROM IF on the top of the APM housing, it will provide connection between APM-2 and APM-1. It will also be directly connected to the EGSE so that camera data packages will be retrieved through its Data IF.

The other core elements are the APM-2 housing and the mounting plate on the bottom of the APM-2. The housing itself is not equipped with a scientific payload. Its functionality is to sustain the upper SIROM IF and make the demonstration more realistic. It contains the SIROM IF controller.

4.2. Interface

With a mass lower than 1,5kg SIROM is a cylinder with an external diameter of 120mm, 30mm height above and 30 mm height inside of an APM. Figure 2 shows SIROM main parts. Due to the need to be operative in planetary missions, the external housing and dust cover prevent contamination that could harm the interface.
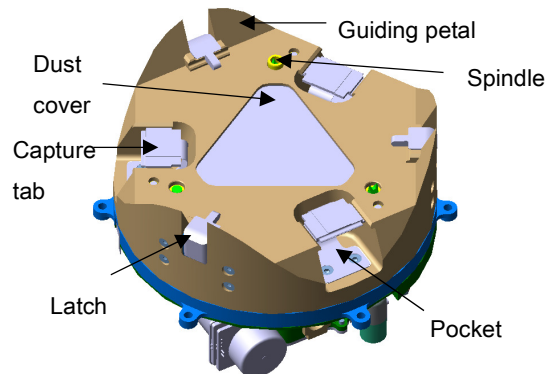

Figure 2 SIROM IF main parts on top of the assembly group (credit: SENER)

SIROMs are directly bolted to APM structure and in general, an APM could be provided with any number of SIROMs. SIROM is provided with holes where the harness for data and electrical transfer pass through, and are to be connected with APM electronics such as payloads, APM controller or other. Apart from that, SIROM presents two elbows for fluid transfer between APM and SIROM interface as shown in Figure 3.

SIROM design not only features mechanical, electrical, data and thermal connections in an integrated and androgynous form, but it also presents main and
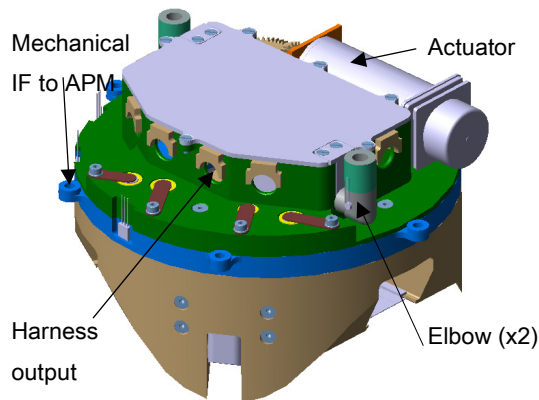
Figure 3 SIROM IF main parts on bottom of the assembly group (credit: SENER)

redundant connections in case one of the lines fails. Electrical, data and thermal IFs are located in the so-called Connectors plate while the mechanical IF is on its own. Figure 4 shows the different functional interfaces.
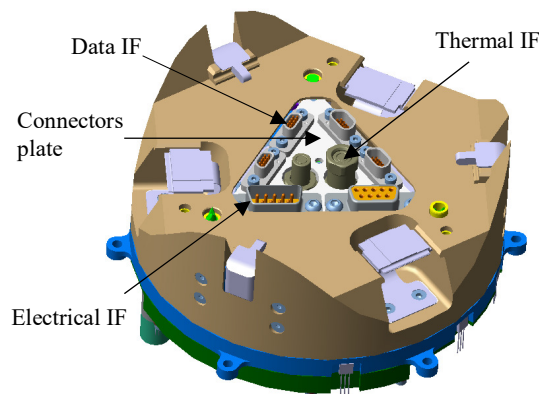

Figure 4 SIROM functional interfaces (credit: SENER)

The main performances of SIROM are summarized in the next table:

Table 1 SIROM performances

Mass	<1,5 kg
Dimensions	128 mm diameter 76,6 mm height
Temperature range	Non-operational: -128ºC to 50ºC Operational: -110ºC to 50ºC
Endurance time	10000 cycles
Voltage power lines	▪ 100 V ▪ 24 V
Electricity transfer	▪ 120 W for 100 V line ▪ 30 W for 24 V line
Data transfer rate	▪ SpW: 100 Mbit/s ▪ CAN: 1 Mbit/s
Heat exchange	2500 W
Power consumption until connection	19 W

Latching force	1020 N
Misalignment tolerance	▪ 10 mm axial ▪ 5 mm other axes ▪ 1,5º all axes
Latching time	60 s
Connection time	102 s
IF to APM	6xM3 bolts at 128 mm diameter circumference
Other performances	▪ Active – Passive SIROM coupling redundancy ▪ Electric, data and thermal lines redundancy

4.3. Structure of the orbital active payload module

As described above an APM is a modular unit, which can be equipped with different assemblies (payloads) providing specific functionality. The basic structure of a standard APM has an outer dimension of 150mm x 150mm x 150 mm, as shown in Figure 5. Depending on the payload, the height can be extended of up to 180 mm. The core structure consists of a cube frame where each side panel is easily detachable while keeping the structure intact. On top and bottom are covers with a retainer for the SIROM IF.

Inside of the housing are slots mounted on two side panels in order to hold the necessary trays. The needed electronic components and payloads can be mounted on the trays.

The detachable side panels allow easy access to the interior for the case of maintenance or repair as long as
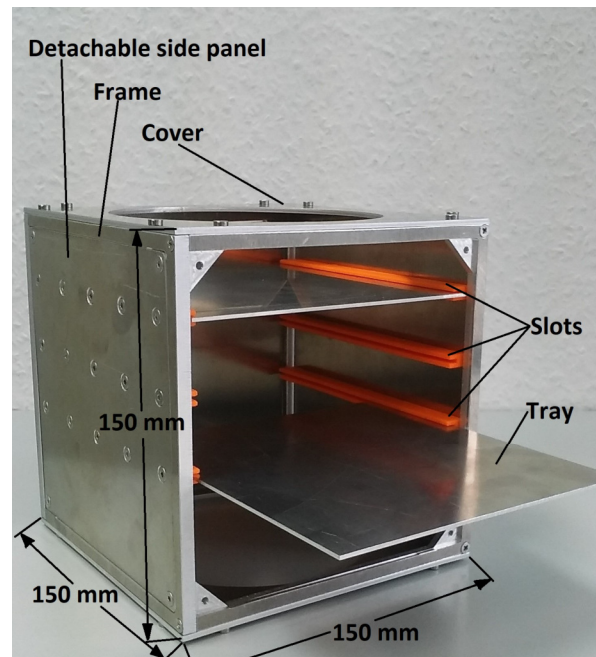

Figure 5 Basic structure of the APM housing(credit: DFKI GmbH 2018)

they are earth demonstrators (first prototypes).The basic structure with frame, side panels and top and bottom cover as well as slots and trays has a weight of 825 g.

Since the scientific orbital APM-1 needs more assembly space for the payload and the components, the height of the basic structure extended up to 180 mm, as shown in Figure 6. The needed trays have openings for the required electronic components in order to avoid accumulation of heat and also openings for the harness routing.

4.4. Approaching and alignment support

For the autonomous robotic handling of the APMs with manipulators it is necessary to determine the relative position of the SIROM interface of the end-effector to that of a payload module to be picked or between the
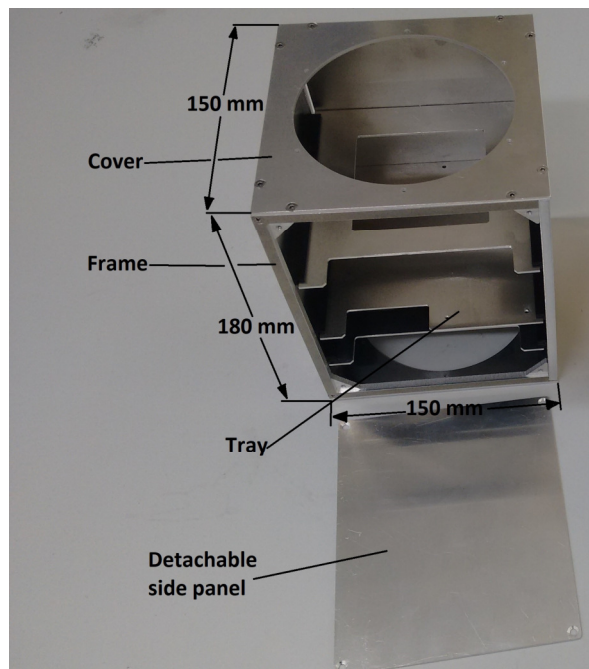

Figure 6 APM-1 with extended height (credit: DFKI GmbH 2018)

interfaces of a payload module which has already been taken by the manipulator and one to which it is to be coupled. For this purpose, ArUco markers are attached to the top of the APMs, which are detected by a camera mounted at the end effector or at the bottom of the APMs. The position of the APM relative to the camera can be determined via the detected markers. This allows the manipulator to position the modules correctly in relation to each other.

However, this visual servoing approach can only be carried out up to a minimum distance of approx. 5 cm. For the last few centimetres, the remaining positioning

error is compensated via force/torque control at the end effector of the manipulator. As support for this last joining step, the surface of the SIROM interfaces has a waveform. This forces the interfaces into the correct position when they are pressed together.

For future orbital missions it is inevitable to use visual servoing during a docking procedure between end-effector and APM, APM and another APM or to servicer and clients.

5. Simulations and Experiment

The main structure of the APM is examined on vibrational modes, to detect eigenfrequencies that can cause resonance problems during launch phase. Based on a finite element approach a structural analysis is performed for frequencies below 2000 Hz, as also practical tests are applied in this region. Thus a modal analysis was performed.

Furthermore experiments in visual servoing were performed in order to find the optimal way of control and calibration. The expected accuracy during the visual servoing operation was ±5mm in x- and y- direction as well as a misalignment angle of 1.5°.

In the SIROM project it was not planned to use visual servoing within the orbital test scenario. For future use of visual servoing also in space applications it is necessary to become familiar with the use of visual servoing. Thus, experiments in visual servoing were performed within equipments tests and also within the preliminary planetary tests. There should be the possibility to transfer the experiences later into the orbital part. The possibility is given since the footprints of both, orbital and planetary APMs, have the same sizes of 150 mm x 150 mm.

5.1. Modal Analysis

A modal analysis of the main structure of the APM housing has been performed, using a finite element method. The underlying model for a finite element is the Bernoulli beam, where shear stresses in the beam are neglected. A free vibration around the equilibrium position (no potential energy is stored internally) without any overall motion (transport kinetic energy is zero) is considered to retrieve the eigenfrequencies. When potential and kinetic energy are linearised, the equation of motion for this case becomes

$$M\ddot{q} + Kq = 0$$

where q is the vector of generalized coordinates, M the mass matrix and K the stiffness matrix of the system. M and K are both symmetric and positive definite. When we replace the vector of generalized coordinates and its second time derivative respectively by

$$q = x \cdot \phi(t)$$

with x as vector of constants and -(t) as any temporal law, Equation 1 becomes

$$\ddot{\phi}(t)Mx + \phi(t)Kx = 0$$

$$Kx = -\frac{\ddot{\phi}(t)}{\phi(t)}Mx$$

Equation 4 defines the general eigenvalue problem of the form

$$(K - \omega^2 M)x = 0 \qquad \text{with} \quad -\frac{\ddot{\phi}(t)}{\phi(t)} = \lambda = \omega^2$$

where λ is its eigenvalue. Since the general solution of an ordinary differential equation under the form is of harmonic type, ω appears to be the circular frequency and is therefore the square root of the eigenvalues. The eigenvector x represents the free vibration shape of the body in every eigenmode.

A model implementation is carried out in the programming language Python to analyse the structure as a wireframe model. The lower part of the structure is clamped (to the launcher) for which the physical properties are given below

Density: 2700 [kg/m³]
Young`s modulus: 68.9·10⁹ [Pa]
Poisson`s number: 0.33
Profile height: 6·10⁻³ [m]
Profile width: 6·10⁻³ [m]

By repeated sub structuring of the wire frame model, the solution for the eigenfrequencies can be obtained from a convergence criterion. In the present case, the sub structuring was interrupted at five subdivisions, presenting an average error of 0.020% and a maximal error of 0.045% to the previous solution regarding all eigenfrequencies below 2000 Hz. The results are shown in Figure 7, where the given numbers indicates modes.
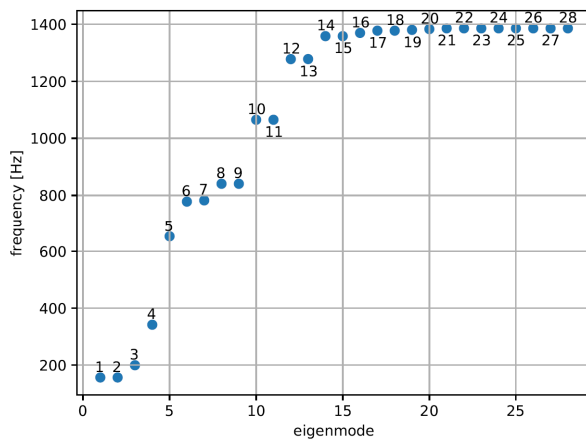

Figure 7 Eigenfrequencies below 2000 Hz

The detected eigenfrequencies are outside the region of harmonic excitation during launch. More detailed investigations regarding random and acoustic vibrations have however to be pursued. The mode shapes of the first four eigenmodes can be seen in Figure 8, showing a qualitative, but not quantitative deflection of the main structure. The simulation results show that the eigenfrequencies are outside the region of sine-excitation of the Ariane launcher. To account for acceptance tests with this launcher, more detailed investigations have to be pursued, as well as real shaker tests.
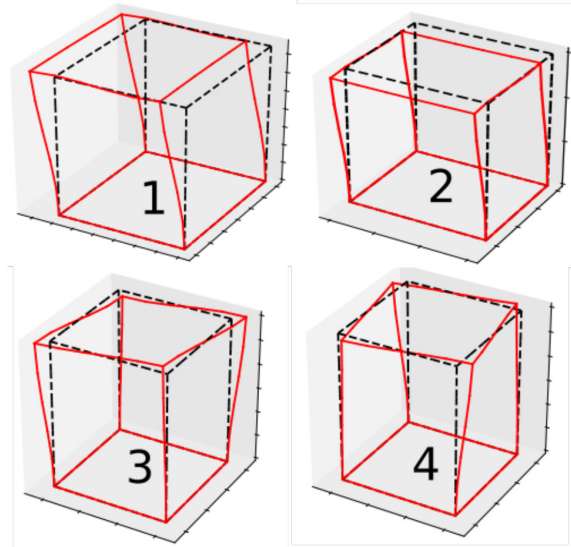

Figure 8 Depiction of the first four eigenmodes, showing the (not to scale) deformations of the structure when bottom nodes are clamped

5.2. Visual Servoing

The task of visual servoing in robotics consists of controlling a pose (assumed here as position and orientation) of an end-effector of a robotic manipulator to reach a target, based on the visual feedback provided by a camera.
Control can be achieved by either using the Position-Based Visual Servo (PBVS) or Image-Based Visual Servo (IBVS). The PBVS uses a calibrated camera and known features of a target object to determine its pose and thus the relative motion necessary to achieve the final relative pose of the end-effector with respect to a target. The IBVS on the other hand uses the image feature extraction directly to derive the required relative motion, without performing pose estimation of the target [4].
The visual servoing control used in the planetary scenario of the SIROM project is the PBVS and was

selected due to its robustness since although the IBVS should be computationally less expensive it presents a challenging control problem due to a highly non-linear relation between the image features and the camera pose [15].

The hardware used for the visual servoing system consists of a Raspberry Pi Zero (used as a control computer) and Raspberry Pi Camera Module v2 (as a visual servoing sensor).

The used software consists of an OpenCV v3.4 with Python 2.7 bindings and custom-made Python modules for the identification of binary square fiducial markers (i.e. ArUco markers) used for the pose estimation of the target surface.

To verify by measurement the performance and limitations of the developed visual servoing system and its control algorithms, three distinct phases were performed and are outlined hereafter:

1. Equipment tests (i.e. development testing at equipment level)
2. Subsystem tests on a testbed (i.e. development testing at subsystem level)
3. Subsystem tests on a robotic platform (i.e. qualification testing at element level)

Testing requirements assumed for the definition of the pass/fail criteria of the aforementioned tests were determined based on the postulated planetary scenario defined within the SIROM project and are the following:

*   The footprint of the APM where a SIROM IF shall be mounted shall not be bigger than 150 x 150 mm;
*   The relative orientation of an APM and its interface shall be detectable via a visual inspection from outside;
*   The visual servoing shall start from a relative distance between the two mating IFs of 200 mm;
*   The robotic arm of the main rover shall be able to achieve an accuracy in position and orientation of ±1 mm and ±0.5 deg, respectively;
*   The mechanical IF shall be able to compensate a relative pose[*] inaccuracy between two mating IFs of ±5 mm and ±1.5 deg;
*   SIROM IFs shall be employed in a space environment, therefore challenging lighting conditions, consisting of hard shadows and areas of extreme brightness/darkness, are to be expected.

---

[*] Defined in this paper as position and orientation.

5.2.1 Equipment tests

The purpose of equipment tests is to ensure the proper functioning of the developed algorithms and equipment and thus validate new design concepts/techniques at the equipment level.

To this end, in this phase of testing the correct implementation of the software onto the Raspberry Pi Zero has been validated along with its capabilities to detect ArUco markers of various sizes and at different distances from the sensor.

The results of the testing outlined the adequacy of the developed hardware-software combination for its intended usage while at the same time pointing out its limitations (e.g. the capability of the system to detect a marker in challenging lighting conditions) that need to be taken into consideration in the next testing phase.

5.2.2 Subsystem tests on a testbed

The scope of subsystem tests on a testbed is to validate new design concepts/techniques at the subsystem level, assess the performance of the visual servoing subsystem in a controlled environment, outline its limitations and provide the input data for the next testing phase.
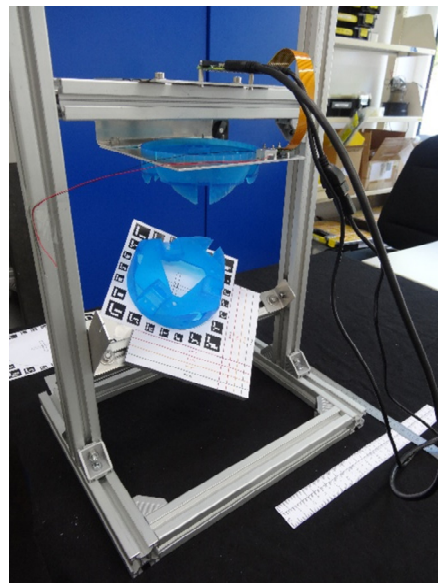

Figure 9 Testbed configuration for subsystem tests of the visual servoing system in bright illumination conditions (credit: DFKI GmbH 2018)

The configuration of the developed testbed, illustrated in Figure 9, consists of a custom-made mounting based on Bosch Rexroth modular profiles, a Raspberry Pi Zero, a Raspberry Pi Camera Module v2, 1-3 Lumileds LUXEON TX SMD LEDs, 2 3D printed SIROM interfaces and a target sheet populated with 4, 12 and 24 ArUco markers.

The tests on a testbed were performed in two different configurations (i.e. baseline and nominal) under

different lighting conditions in order to collect the data regarding the subsystem performance and limitations.

The difference between the baseline and nominal tests consisted of experiments being performed without and with the mounted SIROM interfaces, respectively. The need for two distinct phases has been necessary in order to assess the degree of occlusion of the field of view of the camera originating from the mounted IFs.

Moreover, tests were performed to assess the minimum number of LEDs and their best disposition (see Figure 10) to assure the visibility of markers even in averse/dark lighting conditions.
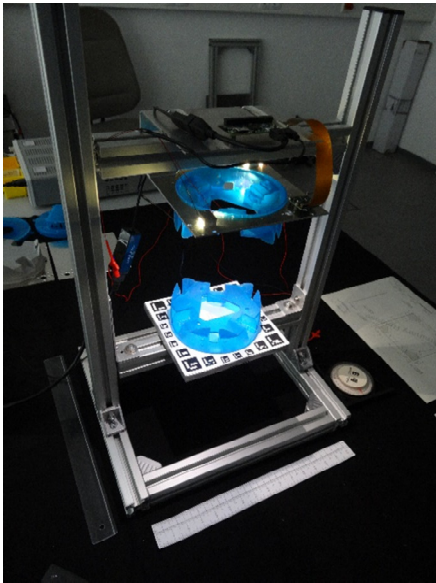

Figure 10 Testbed configuration for subsystem tests of the visual servoing system in dark illumination conditions (credit: DFKI GmbH 2018)

In all of the experiments the relative position and orientation errors of the target w.r.t. the camera were at first considered along different axis separately and then combined in order to assess the capability of the subsystem to detect pose errors. The range of the considered pose errors was between 10-40 mm and 10-40 deg.

The outcome of the tests showed the suitability of the developed visual servoing system to satisfy the requirements of the project and thus the ability of the subsystem to detect relative pose errors of ± 5.5 mm (i.e. ±5 mm + 10 %) and ±1.65 deg (i.e. ±1.5 deg + 10 %).

The tests also pointed out the increase in precision of the subsystem with the greater number of visible ArUco markers on the target surface. This is to be attributed to the fact that some of the visible markers might become undetectable by the subsystem due to occlusions of the interface, its shadow and/or the glare produced by

LEDs. Therefore, a sheet of 24 ArUco markers was assumed as nominal

Regarding the optimum configuration of LEDs on the chaser surface, it was determined that at least one LED, placed near the camera and driven by a DC current of 50 mA is enough to assure the visibility of 9 out of 10 detectable markers in in dark conditions and zero relative pose error between the target and chaser surfaces. This result increased to 10 out of 10 once that LED is coupled with another one placed in one of the adjacent corners of the chaser surface. Therefore it is assumed as the optimum configuration since it would provide redundancy and more robustness.

5.2.3 Subsystem tests on a robotic platform

The scope of subsystem tests on a robotic platform was to perform tests of the subsystem in a real world, robotic platform in a realistic environment to assess the performance of the visual servoing subsystem under challenging conditions and determine its suitability for the usage in the final OG5 tests.

The tests were performed in the Space Exploration Hall of DFKI GmbH and were completed with assistance of a project partner the Space Application Services N.V. (Belgium).

The test equipment used in the tests included:

- SherpaTT rover
- visual servoing subsystem
- mock-ups of the primary and auxiliary APMs (i.e. P- and A-APM)[†], in accordance with the defined planetary scenario.

The rover SherpaTT (see Figure 11) is a hybrid walking and driving rover with an active suspension system developed for high mobility in irregular terrain [16].
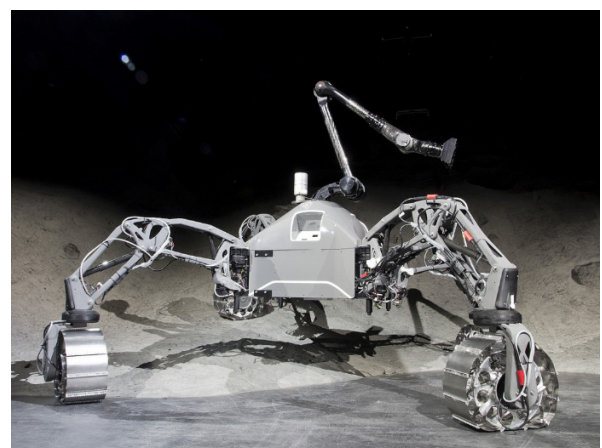

Figure 11: SherpaTT in the Space Exploration Hall of DFKI (credit: DFKI GmbH 2018)

[†] Provided by the Space Application Services N.V. (Belgium).

The rover is equipped with a 6 degrees of freedom (DoF) manipulator, on top of which a mock-up of an auxiliary APM (A-APM), containing a visual servoing subsystem, was mounted, for the eye-in-the-hand configuration, as visible Figure 12.

Figure 12 Docking procedure with PBVS (credit: DFKI GmbH 2018)

A mock-up of a primary APM (P-APM) was used as a target and thus, its upper surface was covered by a target sheet populated with 24 ArUco markers, used as visual aides to the visual servoing system, as illustrated in Figure 12.

The performed preliminary tests consisted all of the following steps:

- align the target and chaser surfaces (i.e. the P- and A-APM) such that mating between the two APMs would be possible via the mounted IFs
- command a pose offset to the A-APM
- perform the PBVS via the visual servoing system
- record the achieved relative pose and compare it to the initial value to obtain the achieved error

The tests were all performed without mounted LEDs and only in bright illumination conditions. However, occlusions and hard shadows of the target surface were present leading in some instances to challenging illumination conditions and necessity to manually illuminate the scene (as visible in Figure 13).

The results of these preliminary tests on a robotic platform have proven in a preliminary way that the developed visual servoing subsystem is able to:

- detect the visual cues on the target surface, even when not in perfect illumination conditions
- detect and correct the relative pose errors almost within the outlined requirements.

Nevertheless, the subsystem did exhibit the necessity of external illumination in conditions of hard shadows. Moreover, the assumed pass criteria, i.e. the ability of the subsystem to detect relative pose errors of ± 5.5 mm (i.e. ± 5 mm + 10 %) and ± 1.65 deg (i.e. ± 1.5 deg + 10 %) have only been met partially. Furthermore, it was noted that the latency between the PBVS command and results output was in the order of 10-15s. Therefore, hardware and software improvements of the visual servoing subsystem are necessary and are under way in the form of LEDs attached to the A-APM, a more efficient 3D hand-eye calibration, and an enhanced communication between the control computer and the subsystem. Further tests should confirm the final adequacy of the developed visual servoing subsystem and document its performance that will be reported in an upcoming paper.
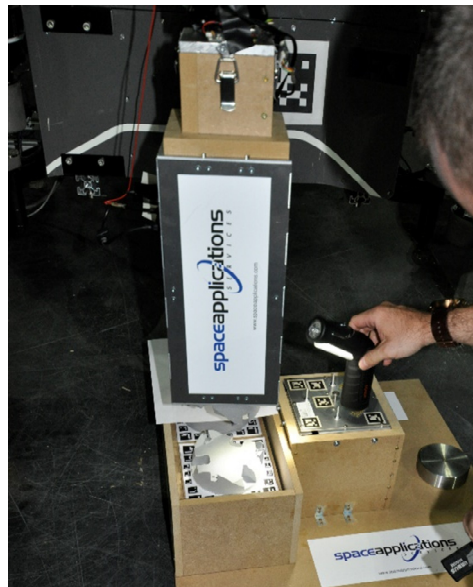

Figure 13 Docking procedure with PBVS and manual illumination of the scene (credit: DFKI GmbH)

6. Conclusion and outlook

The paper describes the structure of the orbital APM housings for the use within the coming orbital test track in order to test the SIROM IF. The housings are able to be attached with two SIROM IFs and necessary components.

One APM-1 is used as a scientific module with a camera, the other APM-2 as mock up for docking of APM-1 The basic structure is 150 mm x 150 mm x 150 mm and ensures a payload of up to 8.5 kg (including the housing). The shapes of the APMs allow the easy handling by a manipulator arm.

The results from the modal analysis show that the main structure of the APM is generally suited for

launches with actual vehicles in terms of sinusoidal excitations.

The test with visual servoing shows the suitability of the developed visual servoing system to satisfy the requirements of the project and thus the ability of the subsystem to detect relative pose errors of ± 5.5 mm (i.e. ±5 mm + 10 %) and ±1.65 deg (i.e. ±1.5 deg + 10 %).
Coming orbital scenario experiments within the Airbus facility, and later at DLR Munich, will prove the design and handling.

References

[1] D. Rossetti, B. Keer, J. Panek, B. Ritter, B. B. Reed, and F. Cepollina, "Spacecraft Modularity for Serviceable Satellites," in *AIAA SPACE 2015 Conference and Exposition*, 2015.

[2] B. Karlow, C. Jewison, D. Sternberg, S. Hall, and A. Golkar, "Tradespace investigation of strategic design factors for large space telescopes," *J. Astron. Telesc. Instruments, Syst.*, vol. 1, no. 2, p. 027003, Apr. 2015.

[3] C. M. Reynerson, "Spacecraft modular architecture design for on-orbit servicing," in *2000 IEEE Aerospace Conference. Proceedings*, vol. 4, pp. 227–238.

[4] M. Jankovic, W. Brinkmann, S. Bartsch, R. Palazzetti, and X. Yan, "Concepts of active payload modules and end-effectors suitable for standard interface for Robotic Manipulation of Payloads in Future Space Missions (SIROM) interface," in *2018 IEEE Aerospace Conference*, 2018, pp. 1–15.

[5] A. A. Kerzhner *et al.*, "Architecting Cellularized Space Systems using Model-Based Design Exploration," in *AIAA SPACE 2013 Conference and Exposition*, 2013, pp. 1–24.

[6] D. Sternberg *et al.*, "A Bottom-up Modeling Approach for the Profit Analysis of Cellularized Spacecraft Architectures," in *64th International Astronautical Congress (IAC)*, 2013, pp. 1–11.

[7] W. Wenzel, R. Palazzetti, X. T. Yan, and S. Bartsch, "Mechanical, thermal, data and power transfer types for robotic space interfaces for orbital and planetary missions - A technical review," in *ASTRA 2017*, 2017.

[8] Wei-Min Shen, R. Kovac, and M. Rubenstein, "SINGO: A single-end-operative and genderless connector for self-reconfiguration, self-assembly and self-healing," in *2009 IEEE International Conference on Robotics and Automation*, 2009, pp. 4253–4258.

[9] M. Christensen, "Phoenix Program. Tools to Tool Changer System Interface Control Document (ICD)," 2013.

[10] W. Wenzel, F. Cordes, and F. Kirchner, "A robust electro-mechanical interface for cooperating heterogeneous multi-robot teams," in *2015 IEEE/RSJ International Conference on Intelligent Robots and Systems (IROS)*, 2015, pp. 1732–1737.

[11] M. Kortman *et al.*, "Building block –based 'iBoss' approach: fully modular systems with standard interface to enhance future satellites," in *66th International Astronautical Congress (IAC)*, 2015, pp. 1–11.

[12] C. G. Henshaw, "The DARPA Phoenix Spacecraft Servicing Program: Overview and Plans for Risk Reduction," 2010.

[13] L. Hill *et al.*, "The Market for Satellite Cellularization: A historical view of the impact of the satlet morphology on the space industry," in *AIAA SPACE 2013 Conference and Exposition*, 2013.

[14] W. Brinkmann *et al.*, "Modular Payload-Items for Payload-assembly and System Enhancement for Future Planetary Missions," in *2018 IEEE Aerospace Conference*, 2018, pp. 1–10.

[15] P. Corke, "Vision-Based Control," in *Robotics, Vision and Control: Fundamental Algorithms in MATLAB®*, 1st ed., B. Siciliano and O. Khatib, Eds. Berlin, Heidelberg, Germany: Springer Berlin Heidelberg, 2011, pp. 455–479.

[16] F. Cordes and A. Babu, "SherpaTT: A Versatile Hybrid Wheeled-Leg Rover," in *In Proceedings of the 13th International Symposium on Artificial Intelligence, Robotics and Automation In Space, (iSAIRAS-16)*, 2016.